Engineering Journal issn: 0125-8281

Article

Evaluation of Building Performance Against Large Subduction Earthquakes Incorporating Ground Response and Structural Dynamics Analysis

Nur Rahman Handayani[a], Lindung Zalbuin Mase[b,*], Sahrul Hari Nugroho[c], Fepy Supriani[d], Rena Misliniyati[e], and Khairul Amri[f]

Department of Civil Engineering, Faculty of Engineering, University of Bengkulu, Bengkulu 38371, Indonesia
E-mail: [a]g1b021083.nurhandayani@mhs.unib.ac.id, [b,*]lmase@unib.ac.id (Corresponding author), [c]sahrulharin02@gmail.com, [d]fsupriani@unib.ac.id, [e]rena_misliniyati@unib.ac.id, [f]kamri@unib.ac.id

Abstract. This study presents an integrated methodology combining ground response and structural dynamics analysis to analyse the earthquake-induced impacts on the resilience of the Integrated Laboratory building at the Faculty of Engineering, University of Bengkulu, during significant earthquakes. The investigation begins by conducting a site characterisation to collect geological data for the study location. A seismic ground response analysis is performed to assess ground motion at the pile tip, followed by the propagation of earthquake waves to evaluate the response of structures to earthquakes. Weak structures are identified through stress ratio evaluation, and retrofitting techniques are applied to enhance their load-bearing capacity. The results indicate that retrofitting has a significant improvement in structural performance. The study highlights the importance of combining ground response and structural dynamics analysis to enhance the safety and durability of buildings in earthquake-prone areas.

Keywords: Earthquake, ground motion characteristics, structural dynamics analysis, retrofit.

ENGINEERING JOURNAL Volume 29 Issue 6
Received 25 March 2025
Accepted 29 May 2025
Published 30 June 2025
Online at https://engj.org/
DOI:10.4186/ej.2025.29.6.59

DOI:10.4186/ej.2025.29.6.59

1. Introduction

Indonesia accounts for almost 10% of worldwide earthquake events [1]. placing it among the most seismically active regions in the world. One of the most significant seismic occurrences was the 2007 Mw 8.6 Bengkulu-Mentawai Earthquake, which caused severe damage and has since become a reference point for seismic design in western Indonesia [2], [3].

Earthquakes from the Sumatra subduction zone have resulted in extensive structural losses, with over 56,000 buildings affected and more than 160 injuries recorded [4]. In addition to being prone to earthquakes, the city of Bengkulu is also prone to flooding in several locations. The history of flooding in Muara Bangkahulu in 2019 has been researched [5].

Many reinforced concrete buildings exhibit high vulnerability to earthquakes, especially in regions with significant seismic risk [6]. particularly in urban and coastal regions with dense populations. Given the ongoing development of public buildings, such as schools, hospitals, and laboratories, ensuring seismic resilience is critical. Compliance with seismic standards such as SNI 1726:2019 is mandatory to minimise life-threatening failures [7], [8].

The Faculty of Engineering's consolidated lab facility at the University of Bengkulu is designed with optimised concrete and steel structures to provide comfort and serve as a facility for education and research. Given its position in an earthquake-prone area, it is essential to know the building's structural performance and safety level during a large earthquake so that it not only provides comfort but also ensures safety. Therefore, the potential damage caused by earthquakes must be considered when planning the construction of multi-storey buildings to minimise damage to the building. Structural buildings must be safe and resilient from seismic damage. This must be taken seriously, given the impact on the safety of many people. Therefore, it is imperative to ensure that building designs comply with seismic codes required by the government.

Minimising potential damage is critical, so structural hazard assessment is urgent [9]. Earthquakes, materials, and location significantly influence a building's performance. If the seismic design code is used to construct a building, it should ensure the safety of the people engaging in activities there. Seismic response analysis can be conducted using finite element modelling to assess how a building performs under earthquake conditions [10]

Seismic design codes play a vital role in ensuring the safety and durability of building structures in earthquake-prone areas. Through mandatory design standards and requirements, these codes aim to mitigate the destructive effects of earthquakes, protect the lives and safety of occupants, and limit damage to building structural elements.

The interaction between dynamic structures and the underlying soil is essential for seismic risk assessment. In this study, the applied method aims to measure seismic vibrations on the ground surface in spectral form using a finite element method (FEM) model [11]. Nonlinear site-specific analyses can be implemented to obtain actual spectral accelerations for structural buildings [12]. The selected ground motion records will be used in a nonlinear dynamic analysis to assess their impact on structural response. This is necessary to view the study's results on earthquake structural resistance [13].

Seismic ground vibration data at the research site is required to evaluate the resistance of building structures to earthquake loads [14]. FEM combines the results of structural dynamic analysis based on the data obtained through seismic response analysis. Seismic response analysis propagates one-dimensional waves into the ground layer beneath the structure, resulting in earthquake-induced motion data. Seismic response analysis propagates one-dimensional waves into the ground layer under the structure, resulting in earthquake-induced ground movement parameters [10].

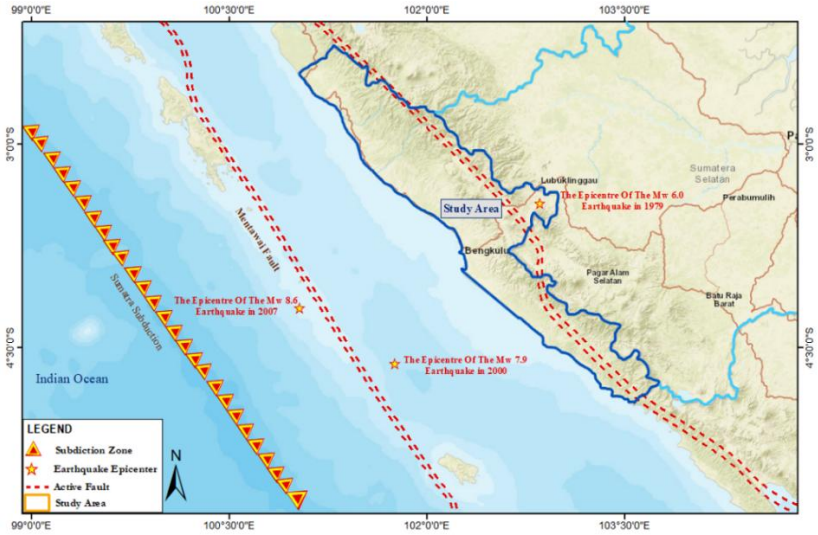

Fig. 1. Map of Tectonic Conditions of Bengkulu Province.

Seismic waves obtain parameters such as ground response and time history data. The analysed results are employed to perform structural dynamic analysis. Time history data and Finite Element Modelling (FEM) can be used to assess structural performance by evaluating ground motion characteristics. Failure patterns in reinforced concrete structures are a crucial aspect that must be thoroughly assessed and understood. Refurbishment is modifying an existing structure to increase its resistance to seismic activity and other natural disasters [15]. During the repair period, it is possible to increase the strength of the structure to design future earthquake-resistant buildings [16].

Earthquakes typically have widespread impacts, necessitating the assessment of building damage on a regional level. Experts should carry out earthquake-building inspections [17]. Seismic evaluation methods include performance-based assessments before and after an earthquake, which are often used to determine whether a structure has been adequately engineered and built to withstand seismic loads. Structural analysis is a decision-making tool used to determine measures to strengthen or demolish structures that do not meet standards. Seismic evaluation and cost-effective rehabilitation are essential to reduce the potential loss of structures and human lives [18].

Implementing retrofit methods is an essential step for weakened buildings [19]. Seismic retrofitting solutions must be effectively designed to improve the existing structures' performance to achieve the specified performance objectives [20]. Retrofitting can minimise the potential for structural failure due to earthquakes. This approach is essential in preventing significant loss of life and severe structural damage. In addition, the method also generates information about the soundness of the monitored buildings or infrastructure, providing a reference for decision-making during an earthquake [21].

Additionally, the Performance-Based Earthquake Engineering (PBEE) method can be employed as an effective solution for assessing and designing building structures that can withstand large earthquakes. PBEE facilitates damage risk assessment through quantifiable performance levels rather than relying solely on approaches that focus on structural strength. This approach also provides flexibility in designing structural systems tailored to the functional requirements and level of risk faced, thereby increasing the adaptability of the design to various disaster scenarios [22].

This paper presents the integrated work for building assessment by combining seismic ground response and dynamic structural analysis. The actual ground motion is propagated. The ground motion parameter is studied. Furthermore, the simulation of dynamic structural analysis is expected to provide a better understanding of the weak structures. The dynamic structural analysis of the improved structures is also performed to check structural performance. In general, this study proposes an integrated method for building assessment as the preliminary stage for adapting to dynamic loads under increased earthquake effects.

2. Theoretical Background and Methods

2.1. Study Area

Figure 2 shows the research site at the University of Bengkulu's Faculty of Engineering Integrated Laboratory Building. Due to its position, it is primarily affected by seismic activity from the Indian Ocean subduction zone. Under this condition, strong earthquakes can potentially occur in this zone.

The Indonesian earthquake-resistant building standards, published in 2017 as SNI 1726:2012, outline the building's construction characteristics. The building utilises reinforced concrete and comprises various structural components, including columns, beams, and slabs, which are depicted in 3D. Figure 3 presents a three-dimensional model of the building structure, which consists of four floors, each measuring 4 meters in height. Generally, three primary materials comprise the subsoils in Bengkulu City: clay, sandy soil, and rock [23].

Fig. 2. Research location map.

DOI:10.4186/ej.2025.29.6.59

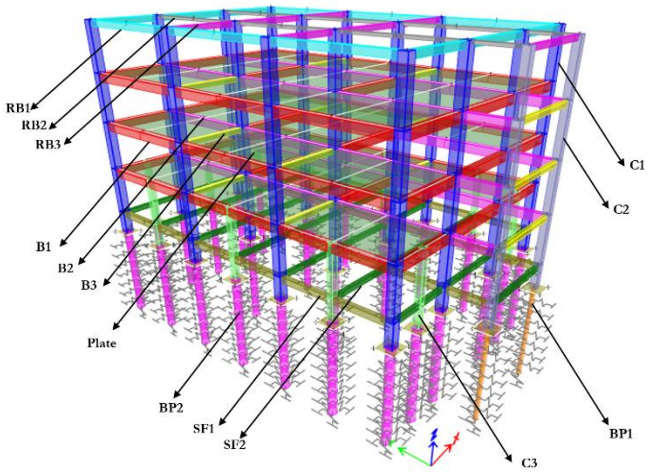

Fig. 3. Research building modelling.

Ground motion is accounted for by utilising seismic recording data. The data collected in this study included site investigation information, such as standard penetration test (SPT) results, shear wave velocities (V_s), and ground motion time histories [24]. The results of this study can support civil engineers in analysing the impact of spatial variation of soil characteristics on geotechnical engineering evaluation through modelling geotechnical parameters such as shear wave velocity (Vs), standard penetration test (SPT) results, soil unit weight (γ), and soil plasticity index (PI) [25]. Seismic tests conducted below ground can measure each soil layer's shear wave velocity [26].

Figure 4 displays the geotechnical data collected from the building site, which outlines essential parameters such as the corrected standard penetration test value (*N-SPT*), shear wave velocity (V_s), unit weight (γ), and plasticity index (*PI*). Standard Penetration Test (SPT) to determine soil density. Higher *N-SPT* values show a positive correlation with increased soil bearing capacity. Plasticity index is a parameter that describes the moisture content range at which the soil is in a plastic condition. The specific gravity of soil serves to determine its physical properties. Shear wave velocity (V_s) is critical in earthquake analysis and geotechnical engineering. High shear wave velocity values correlate with increased soil stiffness, indicating harder and denser soil conditions. V_{s30} refers to the average value of shear wave velocity measured 30 metres below the ground surface.

These parameters are crucial for evaluating soil properties and informing seismic hazard assessments or foundation design. The parameters were utilised when constructing a one-dimensional seismic ground response analysis model in a non-linear state. Organic soils (OH) and dusty clays (CM), which are typically located in the top layer (at shallow depths), are classified as soft soils with low bearing capacity. On the other hand, the values of shear wave velocity (V_s) in the soil layers show an increasing trend with increasing depth [27].

Three typical soil layers exist at the research location. The first, second, and third layers each consist of a clay layer, a sand layer, and a rock layer. The clay part consists of organic clay (OH), plastic clay (CH), and silt clay (CM), extending to a depth of up to 3 meters at the ground surface. The sand layer, located at depths between 3 and 15.2 m, is categorised as SM, silty sand, and SW, well-graded sand. Mase et al. [28] a study focused on Dendam Tak Sudah, identified several soil classifications based on field investigations. The sandy soil at the site was divided into three categories: dusty sand (SM), well-graded sand (SW), and gravelly sand (SG). Meanwhile, the cohesive soil types found in the shallow soil layer consisted of silty clay (CM) and high plasticity clay (CH).

Meanwhile, the rock layer, which consists of weathered sandstone and bedrock, is typically located at depths ranging from 15.2 to 33.9 meters. A stiff layer was detected at a depth of 17.2 m, with an average $(N_1)_{60}$ value of 60 blows per foot. The mean shear wave velocity (V_s) within the upper 30 meters (V_{s30}) is approximately 202 m/s. The engineering bedrock, exhibiting a V_s of 783 m/s, is at a depth of 33.9 meters. Soil variability should be considered to represent soil conditions realistically in the analysis [29]. Since soil properties are strongly influenced by uncontrolled natural processes such as deposition and weathering, their characteristics are highly spatially variable. Therefore, it is important to explicitly consider the spatial variability of soil parameters in numerical analyses to obtain more realistic results [30].

This study employs a finite element-based soil response analysis approach that considers the spatial variability of geotechnical parameters. As Nguyen and Likitlersuang (2021) [31] stated, the spatial variability of soil shear strength can significantly affect the results of structural lateral movement and surface deformation. Hence, a single deterministic approach tends to underestimate or overestimate structural damage.

The spatial variability of geotechnical parameters, such as soil unit weight (γ), plays a crucial role in evaluating seismic response and structural stability. As stated by Nguyen et al. (2024) [32], natural soils exhibit spatial variation of properties, and ignoring the interrelationship of such parameters may result in an inaccurate estimation of design failure risk.

The soil response analysis was performed nonlinearly using the Pressure-Dependent Hyperbolic model, which can capture the dynamic behaviour of layered soils at high strains. Damping values were determined based on the soil type, i.e. 7% for clay and 5% for sand. The model also accommodates the variation of shear modulus with strain, which is essential to reflect realistic ground motion amplification.

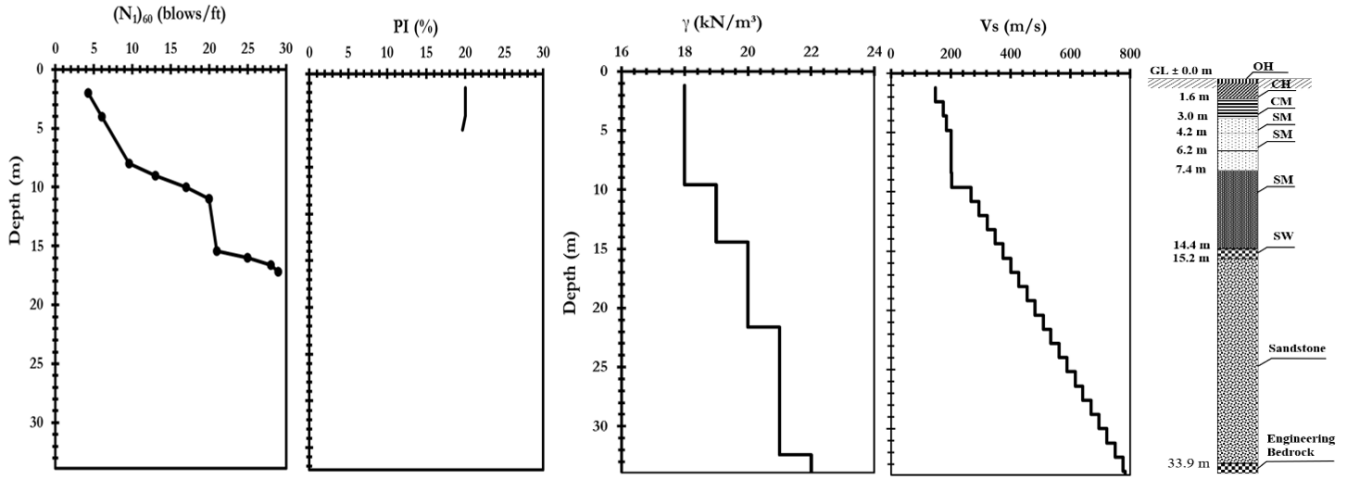

Fig. 4. Site investigation data for the study location.

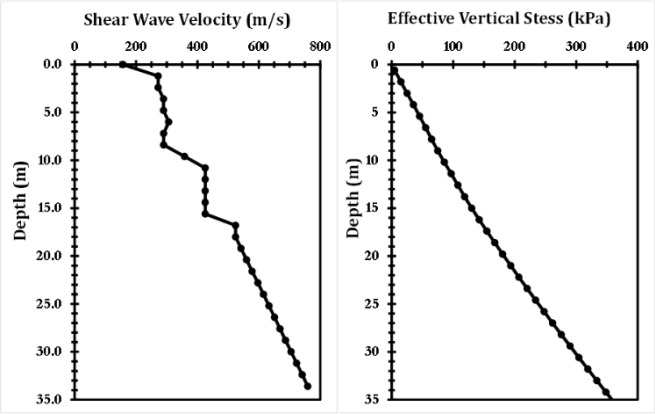

Fig. 5. Shear wave velocity and effective vertical stress.

Input parameters, such as SPT-N (Standard Penetration Test) values and effective vertical stress, were obtained through a field investigation. Figure 5 shows the vertical stress variation in the soil around the bored pile, which is analysed vertically. The effective vertical stress increases with depth until it reaches a specific penetration limit. These stresses represent the load that the soil layer receives from the overlying soil mass, taking into account the influence of pore water pressure.

In this study, one-dimensional (1D) nonlinear soil response analysis, considering effective stress and pore water pressure dissipation, has been applied to investigate the behaviour of layered soils, particularly in terms of peak acceleration and maximum shear stress variations. Simulations were carried out 33.6 metres below the ground surface, concerning the shear wave velocity (Vs). They corrected the N-value (SPT-N value after fine correction) as input parameters to distinguish the characteristics of the soil layers. The shear wave velocity (Vs), calculated from the corrected N value, is shown in Fig. 3 as the velocity profile at the study site.

In addition, ground motion spectra corresponding to the site-specific time history were used in the analyses to simulate the soil's dynamic response to earthquake loads more accurately. This approach ensures that the simulation model represents the real site conditions and the ground's response to earthquake loads.

2.2. Combined Method of Ground Response and Structural Dynamics Analysis

Analysing the performance of buildings in dynamic situations, such as during an earthquake, is crucial. Seismic waves travelling from the bedrock through the ground can profoundly affect the structural stability of buildings. Therefore, evaluating how these waves influence structural performance during seismic events is critical. Table 1 details the structural components of the Integrated Laboratory at the Faculty of Engineering, University of Bengkulu. The characteristics of the building structure are evident from the table.

Figure 6 illustrates the three primary frameworks employed in this study: seismic hazard evaluation, site-specific response analysis, and structural performance during an earthquake. This study uses a one-dimensional nonlinear approach to analyse seismic response, utilising time history analysis as a case study. Several crucial spectral acceleration parameters are involved in the one-dimensional nonlinear analysis of seismic response. These parameters include maximum ground acceleration (PGA) and spectral response acceleration. The results of seismic ground response analyses, which include ground motion time histories and spectral accelerations, are crucial for describing ground response.

These parameters are essential for determining seismic loads with greater accuracy. Ground motion parameters, such as PGA, Amplification Factor (AF), Arias Intensity (IA), and Spectral Acceleration (SA), are derived from seismic wave propagation analysis using the Pressure Dependent Hyperbolic model. Among these parameters, PGA, representing the highest ground acceleration value, is crucial in evaluating the impact of earthquakes of a particular duration [33]. Site response analysis is performed to assess the behaviour of the ground as seismic waves pass through it. This method applies earthquake-induced vibrations from the bedrock upwards through horizontal soil layers. The input motions selected must consider the specific geological conditions

of the site being analysed and the site characteristics of the building.

The finite element method is one of the analytical techniques for the bearing capacity of soils [34]. Three-dimensional finite element method (FEM) is utilised to study the behaviour of buildings during earthquakes. Structural resistance can be evaluated by integrating the calculated parameters with time history data and FEM-based simulations. FEM allows for modelling the reaction of the structure to earthquake forces, assessing the dynamic interaction between the building structure, foundation, and underlying soil. This methodology is coupled with seismic response analysis, which simulates the one-dimensional transmission of seismic waves through soil layers. The results provide essential information on the real-world performance of buildings during seismic activity, enhancing our understanding of how structures interact with the geotechnical environment and respond to ground motions, thereby informing the design of safer and more resilient structures [35].

Time history analysis was chosen because Bengkulu City is prone to earthquakes. The earthquake accelerogram records data from the 12 September 2007 earthquake in the Indian Ocean, which had a magnitude of 8.6 and caused significant damage in Bengkulu Province. The results of this research analysis are essential for evaluating and obtaining information related to the safety of building structures. The stress ratio (R) value can provide information on the structure's safety.

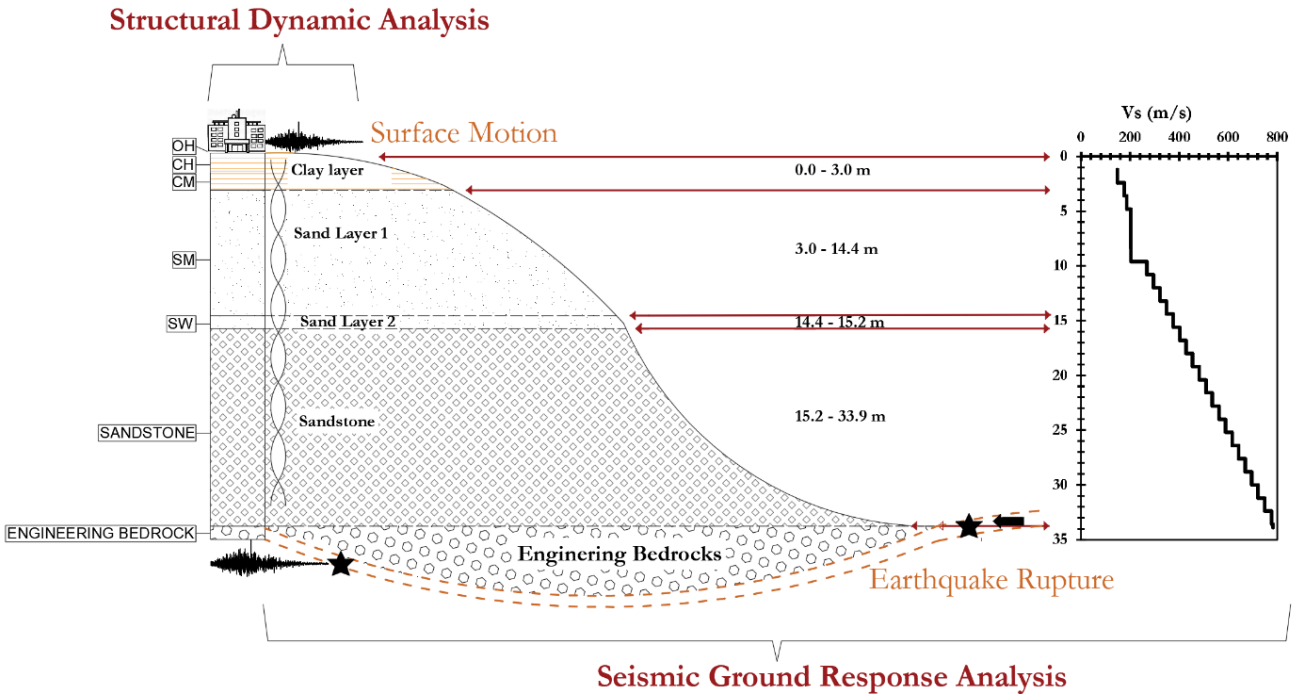

Fig. 6. Schematic of the combined method for structural evaluation (redrawn from Mase [3]).

Table 1. Structural element data.

Structure Elements	Structure Naming	Dimension (mm)	Thickness (mm)
Bore pile	BP1	300	-
	BP2	600	-
Sloof	SF1	250×450	-
	SF2	200×300	-
Column	C1	400×500	-
	C2	400×400	-
	C3	250×250	-
Beam	B1	300×450	-
	B2	300×650	-
	B3	200×350	-
Ring beam	RB1	250×450	-
	RB2	150×350	-
	RB3	150×200	-
Plate	-	-	125

2.3. Performance-Based Earthquake Engineering (PBEE) Approach

PBEE is a method for determining the probability of an earthquake occurrence, a building's response to seismic loads, and potential structural damage. In this research, PBEE can be applied to assess whether the damage caused by a large earthquake remains within the allowable performance levels, such as Immediate Occupancy, Life Safety, or Collapse Prevention, as specified in the FEMA P-58 standard. The PBEE framework serves as a reference to map the relationship between seismic parameters (such as Peak Ground Acceleration/PGA and Spectral Acceleration/Sa) and damage indicators (Damage Index/DI) with the actual level of damage to the building structure. Thus, this approach enables a more scalable and adaptive design for earthquake risk [36].

2.4. Ground Motion Parameter

Seismic wave inputs produce parameters of peak ground acceleration (PGA), peak ground velocity (PGV), Arias Intensity, and cumulative absolute velocity (CAV). Seismic intensities such as CAV, maximum spectral acceleration (*Sa*), *Sa* at a particular period, IA, PGA, etc., comprise various intensity measures [37].

Root Mean Square Acceleration (Arms), this parameter includes the effects of the amplitude of acceleration and duration of ground motion. Root Mean Square Velocity (Vrms) is a parameter that considers the impact of both the amplitude of velocity and the duration of ground motion.

Characteristic Intensity (Ic) is associated with structural damage due to maximum deformation and absorbed hysteretic energy.

Specific Energy Density (SED) represents the energy associated with the velocity-time history of a system.

The Arias intensity assesses ground motion strength by analysing seismic wave acceleration, an essential parameter to characterise earthquake behaviour. The formula (Eq. (1)) defines IA using variables such as gravitational acceleration (g), the duration during which the seismic signal exceeds a threshold (T_d), and acceleration (*a*). This metric is critical in evaluating seismic hazard and understanding earthquake dynamics :

$$IA = \frac{\pi}{g}\int_0^{T_d} a(t)^2\,dt \tag{1}$$

The amplification factor refers to the change, or increase, in ground motion acceleration as it travels from the bedrock to the ground surface. This increase is caused by the difference in shear wave propagation velocity (V_s) between bedrock and soil (sediment) layers. Shear wave velocities (V_s) usually decrease with proximity to the surface, starting from the bedrock. The lower the V_s, the lower the shear modulus (*G*) and damping factor, contributing to increased ground acceleration. The input amplification factor (AF) was evaluated using seismic response analysis. The amplification factor (AF) is determined by comparing the surface acceleration ($PGA_{surface}$) with the acceleration at the pile tip layer (PGA_{input}), which is presented in Eq. (4) as follows [38] :

$$AF_{\max} = \frac{PGA_{surface}}{PGA_{input}} \tag{2}$$

Significant duration refers to intense ground shaking during seismic events, a critical parameter for evaluating structural performance and risk, as well as how structures respond and accumulate damage. This parameter measures the duration of seismic activity that persists beyond thresholds determined by the magnitude and severity of ground shaking, often associated with potential damage from shaking. This duration is quantified by the parameter $D_{5\%IA\text{-}95\%IA}$, which is calculated as the difference between the time (*t*) when 5% of the total IA is accumulated and the time when 100% of the IA) is reached, expressed in the following equation:

$$D_{5\%IA-95\%IA} = t_{95} - t_5 \tag{5}$$

Acceleration Spectrum Intensity (ASI): The area under the acceleration response spectrum between 0.1 s and 0.5 s periods. Velocity Spectrum Intensity (VSI): The area under the velocity response spectrum between 0.1 s and 0.5 s periods.

Sustained Maximum Acceleration (SMA): The third-highest absolute acceleration value in the time history record [39].

Applying damage assessment methodologies and indices (DI) is necessary after an earthquake [40].

Cumulative absolute velocity is derived from integrating (*a*(t)) over time, where (*a*(t)) represents acceleration at the time, as follows [38] :

$$CAV = \int_0^{tf}\left(a(t)^2\,dt\right) \tag{3}$$

2.5. Research Framework

The research is based on the building of the Bengkulu University Faculty of Engineering Integrated Laboratory. It is crucial to examine the seismic performance of the building, as it is located in an earthquake-prone zone, based on the history of the 2007 Bengkulu-Mentawai earthquake. The research combines seismic ground response analysis with structural dynamics analysis, starting with the measurement of field data (Fig. (7)) and the calculation of soil parameters (Table 2). The article utilises ground motion records of the 2007 Bengkulu-Mentawai earthquake, the main scheme in Bengkulu City, to quantify seismic risk and structural impact at a specific location. The input motion time history is presented in Fig. (7). Mase et al. [41] analysed the ground response during a large-scale megathrust earthquake in Bengkulu City using the history of the 2007 M8.6 Bengkulu-Mentawai earthquake. The initial ground motion was modelled at the bedrock surface, then travelled through the soil layers until

it reached the surface. This analysis is essential in predicting ground response during extreme seismic events.

The selection of representative seismic ground motions is crucial for accurate seismic hazard analysis, a step preceding the performance of seismic ground response analysis, which is the subject of this study [42]. The historical records of the 2007 Bengkulu-Mentawai earthquake were analysed using the one-dimensional nonlinear method to evaluate the impact of ground motion and structural response. The secondary data is utilised as input to obtain Peak Ground Acceleration (PGA) values, enabling building inspections under seismic design codes caused by earthquakes [43]. This study propagates seismic waves from the bedrock and through each soil layer. After this propagation process, the ground response can be analysed through several parameters, such as ground motion time histories [44]. Figure 8 indicates the input wave time history utilised in the analysis.

Furthermore, seismic waves are applied for ground motion analysis through the time history analysis method [45]. Moreover, time history analysis is also performed based on PGA and spatial acceleration values, which are then applied to the building model. After all the structural geometry elements of the building are represented, the next step is to input the loading values for the structure, including load cases, load combinations, and mass sources. Time history analysis is carried out to obtain data about the safety of the structure from the stress ratio displayed by the different colours of the structural elements after the dynamic analysis and the internal forces (Normal Force (*N*), Shear Force (*V*) and Bending Moment (*M*)) acting on the building are obtained. Shear forces are used to design the structure to prevent shear failure. Functional regular forces impact the capacity of structural members to resist loads, influencing stability and load-bearing capability [3]. For structural elements that exhibit insecurity or are coloured red and have a stress ratio value greater than one, repairs must be made through retrofitting methods to address weak aspects. The analysis results reveal the structural response regarding normal force, shear force, and bending moment. For safe structures, the results and discussion are continued without retrofitting.

3. Results and discussion

3.1. PGA profile

Seismic response analysis using the hyperbolic model yields several vital parameters, including peak ground acceleration (PGA), spectral response acceleration, and amplification factor. PGA is the peak acceleration as earthquake waves propagate from the bedrock to the Earth's surface and is a crucial parameter for assessing a place's vulnerability to earthquakes. The higher the PGA value, the more damage an earthquake will cause. Additionally, the PGA value provides information on the seismic conditions in a region. It can be concluded that PGA values can be used to describe subduction earthquake situations, aiming to reduce damage to structures during earthquakes [46].

Building performance analysis combines the seismic ground response analysis method with structural dynamics analysis. Geological conditions and ground vibration intensity are the main factors for reinforcement [47]. This method evaluates the structure's response to seismic activity, which is crucial for earthquake-resistant design through spectral analysis [48]. The response spectrum analysis process is carried out by modelling wave propagation using a one-dimensional pressure-dependent hyperbolic nonlinear model. The analysis process in this study begins by compiling soil profiles that aim to generate data related to earthquake acceleration, period, peak spectral acceleration (PSA), frequency, and amplitude. The output of this process is then further processed to obtain seismic parameter values, such as maximum ground acceleration (PGA), spectral response acceleration at short-period intervals (Ss), spectral response acceleration at long-period intervals (S_1), and amplification factor.

Figure 9 displays the PGA (Peak Ground Acceleration) profile from the seismic ground response analysis, indicating that the highest earthquake acceleration is observed at the surface layer, with a peak value of 0.220 g. This layer is predominantly composed of organic clays, underscoring the role of soil type in amplifying ground motion. This condition has the potential to amplify significantly during a large earthquake. This research included the analysis of eight soil layers. The second, third, and fourth layers have PGA values of 0.215 g, 0.208 g, and 0.201 g, respectively. The PGA values in these layers exhibit insignificant differences compared to the surface layer, primarily due to the dominance of silty clay material.

Meanwhile, the fifth to the ninth layers show lower PGA values, 0.192g, 0.181g, 0.170g, 0.159g, and 0.125g. The difference in PGA is quite significant compared to the previous layers because the material that makes up this layer is sandy soil. Layers 10 to 29 have PGA values ranging from 0.121 g to 0.096g. The amplification factor obtained from this study is about 1.430, which reflects the difference in magnification of the earthquake acceleration from the bedrock to the ground surface. This difference is influenced by the value of shear wave velocity (V_s) in each soil layer. The lower the value of shear wave velocity (V_s) at the ground surface, the greater the resulting amplification factor.

3.2. Time History of Ground Motion

Figure 10 displays the time history at the surface, pile tip, and input motion, illustrating the differences from previous studies. In contrast, previous studies have only examined the time history of the input motion. From this study, a peak ground acceleration (PGA) of 0.211 g was observed at the surface layer, a peak ground velocity (PGV) of 0.176 m/s occurred at the same layer, and a peak ground displacement (PGD) of 0.114 m was recorded at the pile tip layer. The acceleration time history shows that the maximum acceleration of the input motion is typically smaller than the acceleration at the ground surface [49].

Table 3 provides the ground movement parameters. Time history ground motion parameters comprise numerous parameters, including spectra, Arias Intensity, and others [50].

The seismic ground motions generated by the most influential earthquakes in the study area are used to predict the performance of building structures during earthquakes. Misliniyati et al. [51] conducted similar research in Bengkulu City. Based on the results of their study, the ground motion parameters obtained are as follows: the maximum acceleration (PGA_{max}) is 0.154 g, the maximum velocity (PGV_{max}) is 0.124 m/s, and the maximum displacement (PGD_{max}) is 0.097 m. The short period indicates that this movement can have a significant impact on low-rise buildings. The short period suggests that this motion can have a dramatic effect on low- to medium-rise buildings.

3.3. Spectral Acceleration

Ground motion prediction analyses are performed to determine spectral acceleration values, which are then used to simulate the relevant ground motions at each location [52]. Figure 11 illustrates the spectral acceleration graphically. The seismic response analysis of the ground reveals that the peak spectral acceleration is observed at the ground surface. The study showed that spectral acceleration values recorded at the ground surface exceeded those predicted by seismic site-response modelling; a similar finding was also reported in Qodri et al. [53].

Conducted in Banten Province, the study found that the spectral acceleration at the input motion is lower than at ground level, indicating that the input motion is amplified. Spectral acceleration curves for the surface layer and pile tip are also generated based on the evaluation of ground motions caused by earthquakes, including acceleration time histories. These curves were evaluated against the design spectral acceleration specified in SNI 1726:2012, the reference standard for building design, and SNI 1726:2019, the latest code applied to all construction projects since 2019. Previous research has been conducted on the value of spectral acceleration in the sports building of Bengkulu University. For comparison purposes, a study was conducted by Mase et al. [3].

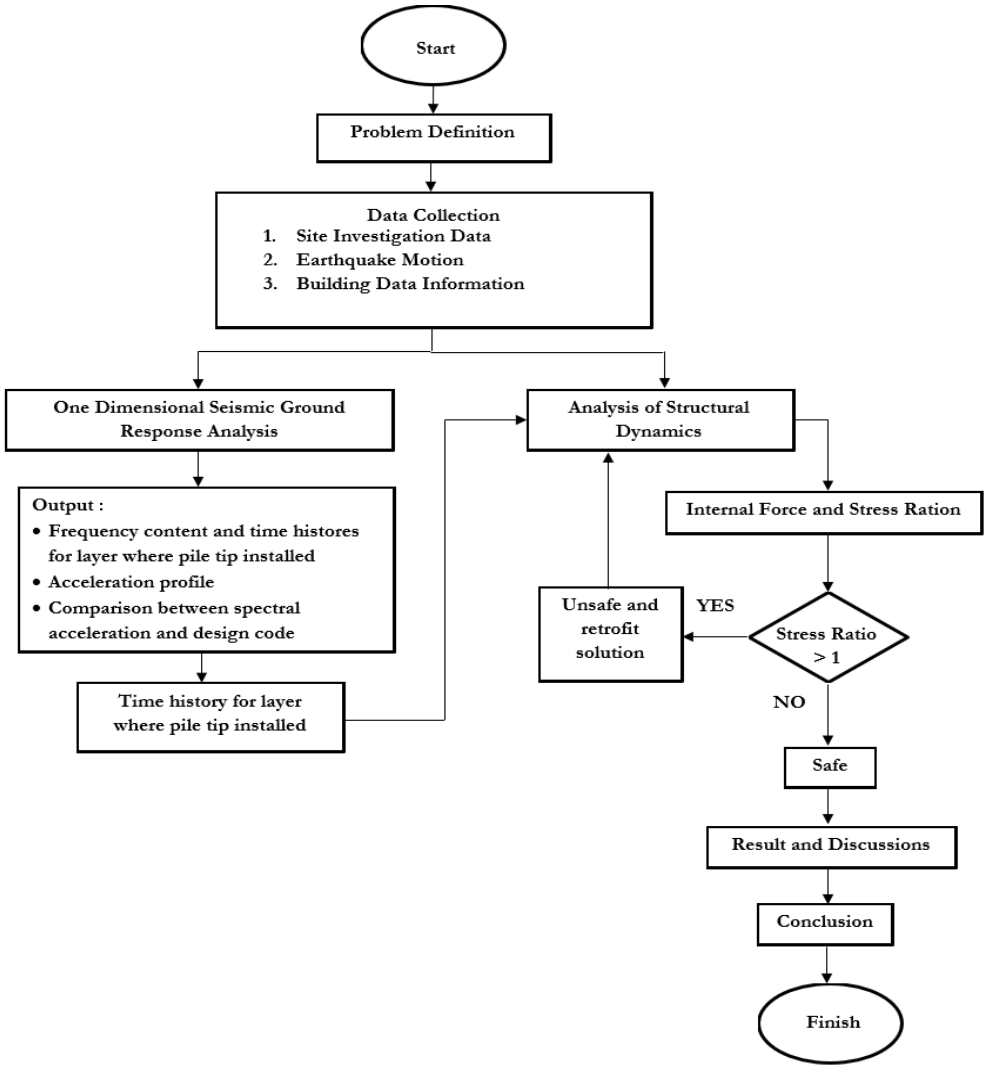

Fig. 7. Research flow chart.

DOI:10.4186/ej.2025.29.6.59

Table 2. Soil modelling input parameters.

Layer	h(m)	V_s (m/s)	γ (kN/m3))	Damping Ratio (%)	Ref. Stress (MPa)
Clay	1.200	147.580	18.400	0.960	0.180
Clay	1.200	176.120	18.270	0.960	0.180
Clay	1.200	176.120	17.920	0.960	0.180
Clay	1.200	186.430	17.890	0.960	0.180
Sand	1.200	202.230	18.010	0.940	0.180
Sand	1.200	202.230	17.870	0.940	0.180
Sand	1.200	202.230	17.750	0.940	0.180
Sand	1.200	203.020	17.660	0.370	0.180
Sand	1.200	268.150	18.580	0.370	0.180
Sand	1.200	294.870	18.850	0.370	0.180
Sand	1.200	321.590	19.090	0.370	0.180
Sand	1.200	348.310	19.310	0.370	0.180
Sand	1.200	375.030	19.520	0.370	0.180
Sand	1.200	401.750	19.720	0.370	0.180
Sand	1.200	428.470	19.900	0.370	0.180
Sand	1.200	455.190	20.070	0.370	0.180
Sand	1.200	481.910	20.230	0.370	0.180
Sand	1.200	508.630	20.390	0.370	0.180
Sand	1.200	535.350	20.530	0.370	0.180
Sand	1.200	562.070	20.670	0.370	0.180
Sand	1.200	588.790	20.810	0.370	0.180
Sand	1.200	615.510	20.930	0.370	0.180
Sand	1.200	642.230	21.060	0.370	0.180
Sand	1.200	668.950	21.170	0.370	0.180
Sand	1.200	695.670	21.280	0.370	0.180
Sand	1.200	722.390	21.390	0.370	0.180
Sand	1.200	749.110	21.500	0.370	0.180
Sand	1.200	775.830	21.600	0.370	0.180
Sand	0.300	782.610	21.600	0.370	0.180
Sand	1.200	695.670	21.280	0.370	0.180
Sand	1.200	722.390	21.390	0.370	0.180
Sand	1.200	749.110	21.500	0.370	0.180
Sand	1.200	775.830	21.600	0.370	0.180
Sand	0.300	782.610	21.600	0.370	0.180

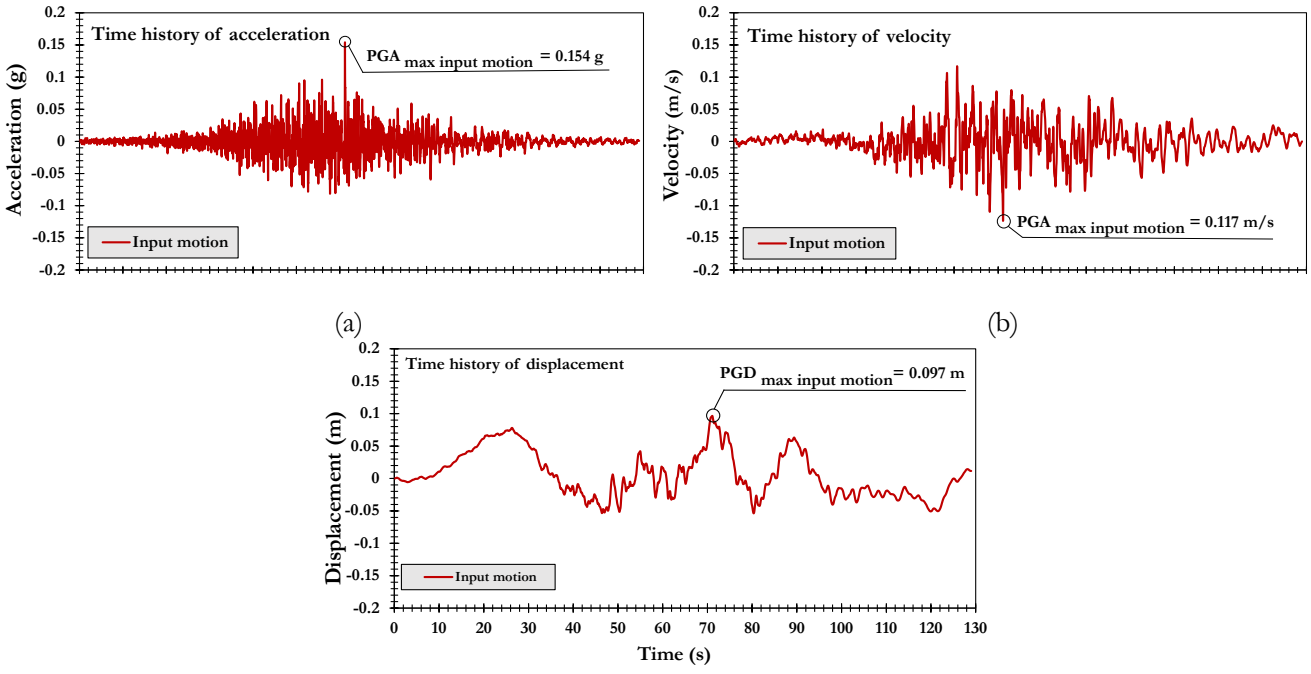

Fig. 8. Time history of Input motion (a) acceleration, (b) velocity, (c) displacement.

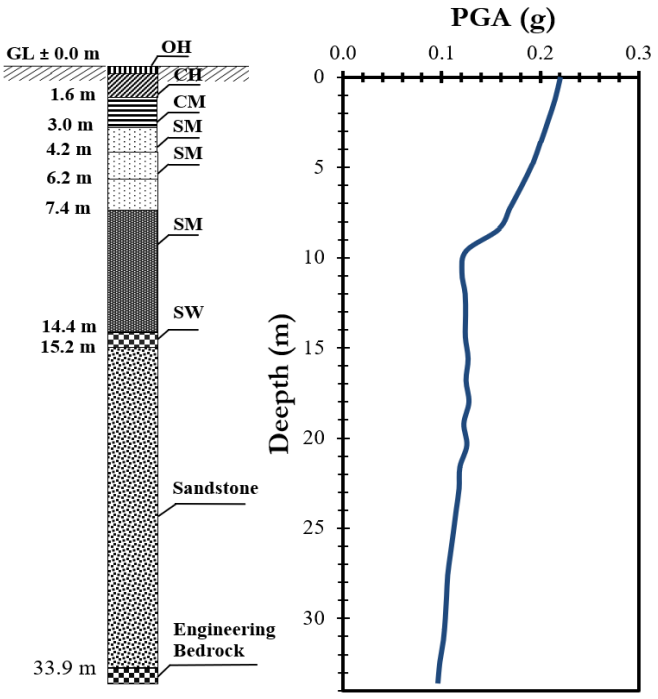

Fig. 9. Profile of peak ground acceleration (PGA) from ground response analysis results.

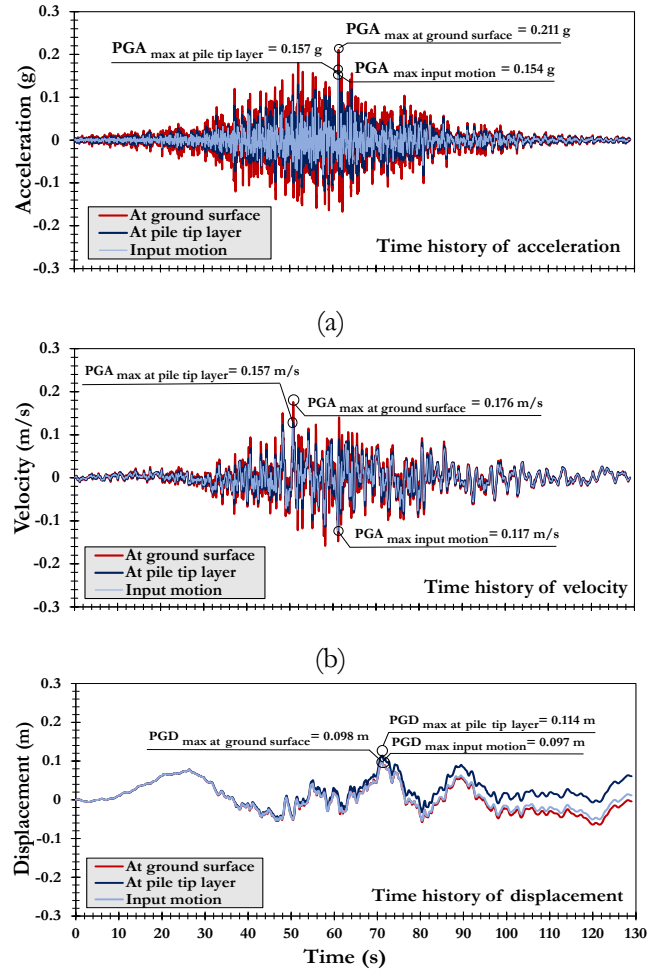

Fig. 9. Time history of ground motions at ground surface, pile tip layer, and input motion for (a) acceleration, (b) velocity, (c) displacement.

In that analysis, the spectral acceleration occurred at a period of 0.3 to 0.5 s, which shows similarity with the spectral acceleration found in this study. $T_n = 0.1N$ is the formula for finding the natural period of the building (T_n). n is the number of storeys, indicating that structural resonance could arise at the investigated site, particularly in the case of mid-rise buildings, as their natural periods will match those of significant ground shaking.

It should be noted that the building is constructed before 2019. It indicates that the standard for the building is still SNI 1726-2012. Based on SNI 1726:2019 standards, the spectral acceleration values for Bengkulu City tend to be higher than those in the foundation layer and input motion. This research demonstrates that the Integrated Laboratory Building of the Faculty of Engineering, University of Bengkulu, meets the standards of the established design code, yielding relatively safe results in the event of earthquake shaking. However, the spectral acceleration at the ground surface is generally higher than the spectral acceleration design for the medium period. It should also be concerned about the building.

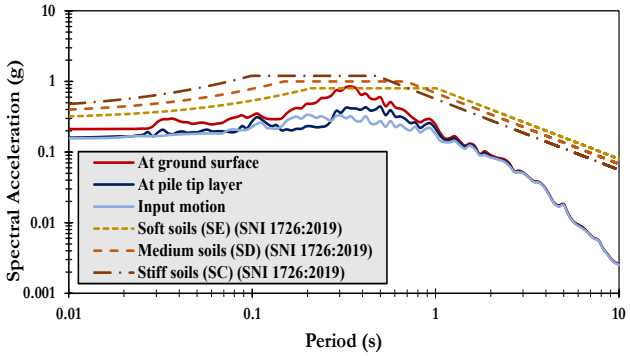

Fig. 11. Spectral acceleration comparison.

This can be seen from the value of spectral acceleration in the ground surface layer, which is almost comparable to the seismic design code established by the Indonesian government for seismic-resistant design planning of building and non-building structures, as outlined in SNI 1726:2012 and SNI 1726:2019.

3.4. Arias Intensity and Duration Significant

Figure 12 shows the time history of the Arias intensity and duration for the pile tip layer acceleration and duration at ground level. As shown in Fig. 10, according to the analysis, the significant duration of the ground motion at the input motion is approximately 49.65 seconds. Compared to the duration at the pile tip layer, which is approximately 46 seconds, the duration at the ground surface is approximately 44.35 seconds. In general, it can be concluded that the pile tip layer tends to have a longer significant duration than at the ground surface. The results also showed a significant reduction in duration from the input motion to the ground surface. Based on the simulation, there is a 5.3-second reduction of the substantial duration from the input motion to the ground surface.

DOI:10.4186/ej.2025.29.6.59

3.5. Dynamic Response of the Building

Finite element modelling was performed to analyse the building's response to various loads, including permanent static forces (e.g., building materials), temporary variable forces (e.g., occupants or furniture), and seismic stresses caused by ground movements during earthquakes. The process of examining the performance of the Integrated Laboratory Building at the Faculty of Engineering, University of Bengkulu, follows the guidelines contained in Indonesian National Standard 1726:2019, which regulates the procedures for earthquake-resistant planning of building structures. After the modelling and analysis of the structure is complete, the next step is to check the structure's performance in the face of earthquake loads, one of which is through checking the mass participation of the building structure. The modelling and analysis of the structure also require checking the mass involvement in various vibration modes. The mode shape is the pattern that arises due to the wobble of the building structure.

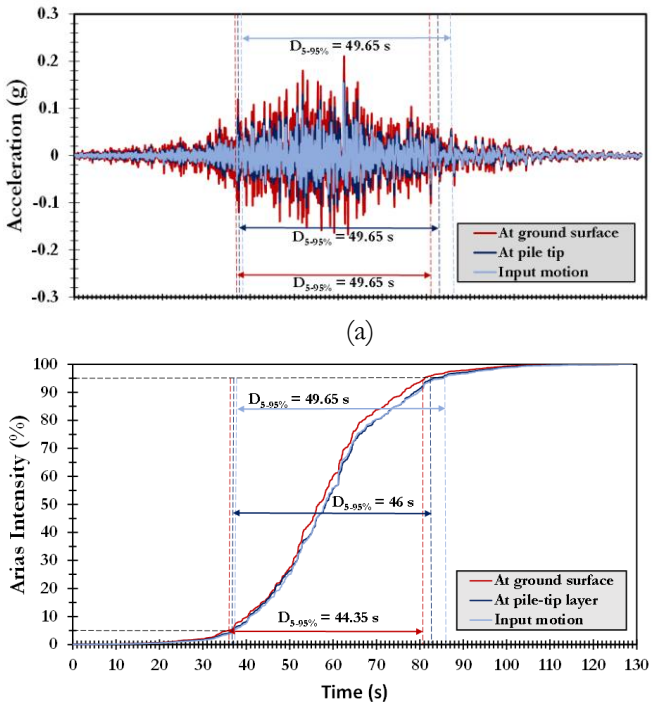

Fig. 12. Correlation between acceleration for significant duration and Arias Intensity (a) acceleration for significant duration, (b) Arias Intensity.

Table 4 summarises the variation in mass participation, covering translational (first and second) and rotational (third) directions for the building performance analysis. Utilising 200 vibration modes, the study achieved 100% mass participation, ensuring a comprehensive analysis of earthquake forces by SNI 1726:2019 standards. The structural analysis results in this study indicate that the first vibration pattern in the building exhibits a mode shape that experiences a translation of 0.738 seconds, moving towards the x-axis. The second building's vibration pattern (mode shape) yielded a value of 6.81 s, indicating that the building experienced a translation towards the y-axis. The first and second vibration patterns do not show rotation. In contrast, the third vibration pattern shows the building experiencing rotation that moves towards the x and y axes with a vibration pattern value (mode shape) of 0.585 s.

The research also assessed internal forces before and after the application of load (Fig. 13). Figure 13(a) illustrates the standard force diagram, showing how earthquake loads affect the components within the Integrated Laboratory Building at the Faculty of Engineering, Bengkulu University, with forces aligned along the structural bars. The structure of the building affects the value of the normal force; the more significant the cross-sectional area, the higher the normal force value. Figure 13(b) shows the shear force diagram of the force results in the building structure after the earthquake load is applied. This shear force diagram illustrates the value on the bar axis resulting from the reaction between perpendicular structural elements. Figure 13 (c) illustrates the moment diagram of the resulting forces in the building structure after applying earthquake loads. This moment diagram shows that the cross-sectional dimensions of the structure influence the values.

The internal force values were obtained through structural analyses using the finite element technique. Table 5 presents a summary of the maximum internal forces in the building structure before the application of earthquake loads. The resulting normal force varies between 6,693 and 770,270 kN. Shear forces were also diverse, ranging from 0.639 to 156.113 kN, while maximum moments ranged from 1.204 to 177.953 kNm. The seismic response analysis provided a summary of the maximum internal forces in all structural elements after the earthquake. The resulting normal force varies from 6,931 to 1,045,924 kN; the shear force ranges from 0,620 to 225,714 kN, and the maximum moment from 1,013 to 296,838 kN. Internal force using acceleration time history analysis showed a clear difference between before and after the earthquake load was applied. The internal force values generated before the earthquake load were smaller than those generated after the earthquake load was applied. Therefore, the earthquake acceleration values input into the building structure affect the internal force values generated within it.

Table 5 presents the percentage increase in internal forces resulting from the applied earthquake loads. For the normal force, the percentage increase ranged from 4 to 82%. For shear forces, the increased values ranged from 0 to 248%. Regarding bending moment, the percentages ranged from 0 to 195%. After the earthquake load is applied, the moment and shear force of the structure may decrease or increase, depending on the structural response mechanism and earthquake characteristics. Decreased moments typically occur when a structure can absorb seismic energy, such as a building designed to be flexible, thereby minimising force transfer to the structure. An increase in moment occurs when the structure cannot absorb energy effectively, such as a rigid structure, so the moment will be larger and may cause damage.

Table 3. Ground Motion Parameters.

Parameter	Input motion	At pile tip layer	At ground surface	Unit
Max Peak Ground Acceleration (PGA_{max})	0.154	0.157	0.211	g
Time of PGA_{max}	61.170	61.350	61.340	s
Max Peak Ground Velocity (PGV_{max})	12.355	12.712	17.607	cm/s
Time of PGV_{max}	61.110	50.780	50.790	s
Max Peak Ground Displacement (PGD_{max})	9.653	11.423	9.774	cm
Time of PGD_{max}	71.090	71.150	71.170	s
PGV_{max}/PGA_{max}	0.082	0.083	0.085	s
Acceleration Root Mean Square (A_{RMS})	0.017	0.022	0.035	g
Velocity Root Mean Square (V_{RMS})	2.415	2.662	3.090	cm/s
Displacement Root Mean Square (D_{RMS})	3.558	3.982	3.761	cm
Arias Intensity (IA)	0.581	0.970	2.464	m/s
Characteristic Intensity (I_c)	0.025	0.037	0.075	-
Specific Energy Density (SED)	752.205	914.207	1231.628	cm^2/s
Cumulative Absolute Velocity (CAV)	1327.068	1729.785	2745.225	cm/s
Acceleration Spectrum Intensity (ASI)	0.114	0.132	0.234	g·s
Velocity Spectrum Intensity (VSI)	60.703	69.662	85.282	cm
Housner Intensity (HI)	58.164	65.257	76.114	cm
Sustained Maximum Acceleration (SMA)	0.095	0.120	0.167	g
Sustained Maximum Velocity (SMV)	10.960	12.230	15.033	cm/s
Effective Design Acceleration (EDA)	0.157	0.145	0.208	g
A_{95} parameter (g)	0.067	0.085	0.127	g
Predominant Period (T_0)	0.200	0.500	0.340	s
Mean Period (T_m)	0.630	0.566	0.430	s
Max Incremental Velocity (MIV)	17.319	21.247	28.844	cm·s
Damage Index (DI)	0.735	1.261	3.216	-
Number of Effective Cycles (NEC)	8.782	11.202	15.421	cycles
Impulsive Index (IP)	108.741	136.683	155.302	-
Average Spectral Acceleration (SA_{avg})	0.142	0.158	0.188	g
Standardised CAV ($Std\text{-}CAV$)	0.674	1.089	2.156	g·s

This demonstrates the critical role of column C3 in resisting the heightened forces and bending moments induced by the earthquake. During seismic shaking, the horizontal loads on the building caused the normal force on C3 to double compared to the static load conditions.

Additionally, SF2 weakened as the beam could not withstand the applied load, weakening the structure. The bending moment in SF2 declined post-earthquake relative to baseline measurements. As the primary beam linking pile caps, the seismic moments proved more consequential, underscoring the importance of strengthening the pile cap-to-beam interface for improved seismic performance.

Therefore, it is essential to investigate the stress capacity and stresses received to determine if structural repairs are required. The information on structural safety in this study is divided into two parts, namely, the evaluation of structural safety before and after the application of earthquake loads.

The evaluation results indicate that the building had sufficient strength before the earthquake load was applied, as all structural elements met the design requirements, with all concrete elements passing the design check. The design check is also performed for all purposes, especially at the design, construction, and operation stages. These regular inspections are addressed to ensure the building has fulfilled all requirements and conditions.

Figure 13 shows the stress ratio distribution of the structure to which the earthquake load was applied. If the stress ratio is more significant than one, dimensional adjustment should be considered. Structural strengthening measures should be taken if this occurs in an existing building.

Simulations on the structure of the Integrated Laboratory Building of the Faculty of Engineering, University of Bengkulu, were conducted by applying earthquake loads obtained from seismic response analyses. The results of the structural response after incorporating the earthquake acceleration time history show that some elements are coloured red and O/S, indicating that the Faculty of Engineering's research facility at the University of Bengkulu is overstrength or unsafe.

Figure 14 also indicates that the beams are experiencing structural weakness, as indicated by the red line. Element B2 was overstressed and thus became unsafe. From the finite element analysis, the beam element exhibited a structural deficiency, with the resultant shear stress exceeding the maximum permissible design limit.

In the structural analysis, 200 vibration shape modes were used to ensure that the total mass participation exceeds 90% in both the X and Y directions, as per the provisions of SNI 1726:2019. The time history results indicate an increase in internal force and bending moment in the beam type SF2 and column C3, which are further classified as critical elements based on a stress ratio greater than 1.

Based on the PBEE principle, structural elements such as column C3 and sloof SF2 with a stress ratio exceeding 1 (>1) are classified at the Collapse Prevention performance level as shown in Table 6. Meanwhile, the Life Safety performance level encompasses other elements that remain within the safe range. This division of performance levels is crucial in designing effective retrofit intervention strategies to maintain or improve the building's functional capability after an earthquake. Classification by PBEE ensures that structural repair priorities are aligned with the risk and performance targets set, such as Immediate Occupancy or Collapse Prevention standards in FEMA P-58 guidelines.

This study presents a novel integration between nonlinear site response analysis and dynamic evaluation of structures based on real earthquake inputs, framed within the Performance-Based Earthquake Engineering (PBE) approach. Unlike previous studies that stop at quantifying structural response, this study incorporates damage assessment indicators (e.g., stress ratio and Damage Index) and proposes specific retrofitting strategies based on observed weaknesses. This study provides a performance-based framework that can be applied to subduction-prone regions with similar geotechnical profiles.

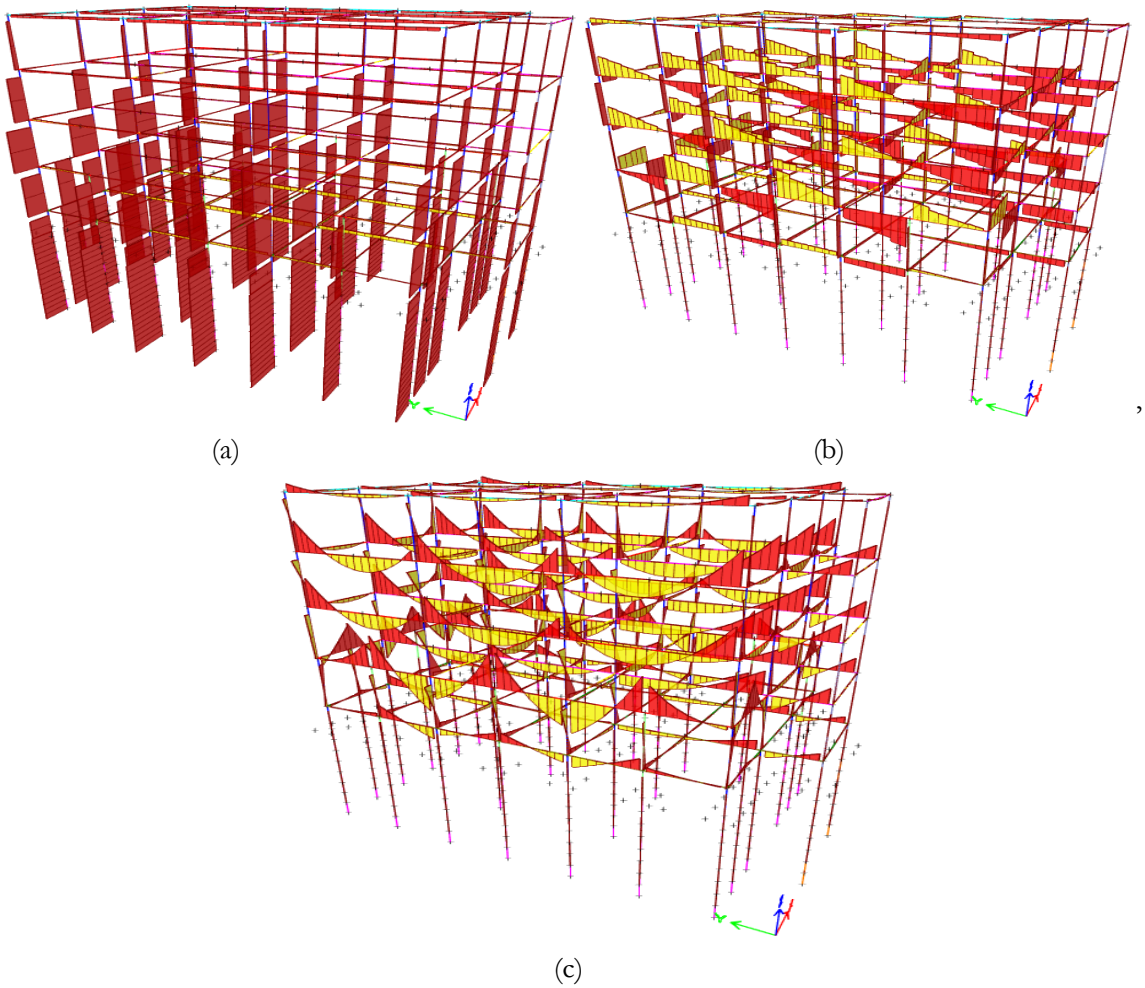

Fig. 13. Internal forces under earthquake load, (a) normal forces, (b) shear forces, (c) bending moment.

Table 4. Mode shape and mass ratio.

Mode	T (s)	U_X	U_Y	R_Z	SUM U_X	SUM U_Y	SUM R_Z	Information
1	0.738	0.860	0	0	0	0.121	0	Translation x
2	0.681	0	0.868	0	0.110	0.121	0	Translation y
3	0.585	0	0	0.854	0.110	0.122	0.845	Rotation z

Table 5. Assessment of structural forces before and after seismic loading.

Elements	Maximum Element Strength						Percentage Difference %		
	Before			After					
	Normal Force (kN)	Shear Force (kN)	Moment (kNm)	Normal Force (kN)	Shear Force (kN)	Moment (kNm)	Normal Force (kN)	Shear Force (kN)	Moment (kNm)
Sloof 1	77.608	43.776	61.227	111.180	64.999	102.824	43%	48%	68%
Sloof 2	58.799	36.658	54.502	61.214	34.913	47.433	4%	-5%	-13%
Beam 1	23.157	156.113	177.953	40.883	225.714	296.838	77%	45%	67%
Beam 2	35.994	98.514	192.855	54.782	133.621	261.533	52%	36%	36%
Beam 3	6.693	25.507	32.289	6.931	46.785	42.030	4%	83%	30%
Ring Beam 1	36.88	18.378	32.989	67.004	32.227	57.675	82%	75%	75%
Ring Beam 2	41.100	12.464	21.893	48.133	19.066	26.600	17%	53%	22%
Ring Beam 3	40.028	4.353	6.748	62.652	15.150	19.888	57%	248%	195%
Column 1	673.352	47.649	91.278	949.006	55.403	103.715	41%	16%	14%
Column 2	327.798	4.209	8.388	458.683	5.394	11.107	40%	28%	32%
Column 3	397.255	27.286	46.594	621.801	23.664	42.487	57%	-13%	-9%
Bore Pile 1	368.753	0.639	1.204	499.638	0.620	1.013	35%	-3%	-16%
Bore Pile 2	770.027	2.309	9.104	1045.924	2.409	6.605	36%	4%	-27%
Pile Cap	-	5.824	16.124	-	5.824	16.124	-	0%	0%
Floor Plate	-	36.371	28.177	-	41.228	48.058	-	13%	71%

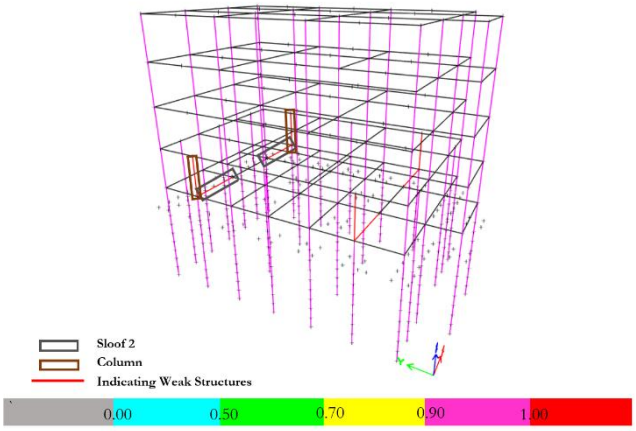

Fig. 14. Stress ratio of concrete structure.

Table 6. Performance-Based Earthquake Engineering (PBEE) Level.

Elements	PBEE Level
Bore Pile 1	Life Safety
Bore Pile 2	Life Safety
Sloof 1	Life Safety
Sloof 2	Collapse Prevention
Column 1	Life Safety
Column 2	Life Safety
Column 3	Collapse Prevention
Beam 1	Life Safety
Beam 2	Life Safety
Beam 3	Life Safety
Ring Beam 1	Life Safety
Ring Beam 2	Life Safety
Ring Beam 3	Life Safety

4. Retrofitting

After assessing a building's seismicity and mapping its shortfalls, remarkable rehabilitation goals must be customised. Seismic retrofitting designs must be implemented effectively to enhance the original building's performance and meet the performance requirements defined by the design code. The analysis revealed structural failures in eight elements of the Integrated Laboratory Building at the Faculty of Engineering, University of Bengkulu. The structural elements considered unsafe are column 3 and slot 2, which experienced loads exceeding the initial capacity, resulting in deflections and cracks in the building. In particular, it is imperative to ensure that buildings have adequate capabilities in the face of recurring natural disasters.

This is because secondary and tertiary earthquakes can have a significant impact on structural performance. One strategy to improve the performance of columns and slots is to reinforce and repair them through retrofitting methods. The retrofitting method involves adding new structural components to an existing building system and applying a layer or strip of fibre-reinforced polymer (FRP) to the wall surface, which is then coated with epoxy resin.

FRP technology was initially developed for structural rehabilitation, with examples including applications in existing bridge structures and seismic retrofitting of constructions, both before and after earthquake events. FRP technology offers several advantages, including increasing the flexural capacity of slabs and beams, enhancing the shear capacity of beams, and improving the standard and shear capacity of columns. Fibre Reinforced Polymer (FRP) sheets offer a high strength-to-weight ratio

DOI:10.4186/ej.2025.29.6.59

and notable anti-corrosive properties. Additionally, the out-of-plane flexibility of FRP sheets offers advantages in their application to various cross-sectional shapes, simplifying the construction process. The relatively high construction speed is also a plus in renovation and repair projects for building, since it would also be effective, efficient, and economic [54].

Figures 15 and 16 illustrate the addition of new structural components to beams and columns. Concrete coating is a popular and conventional method for reinforcing reinforced concrete (RC) elements, such as beams, columns, shear walls, and foundations. The strength and ductility of such parts can be increased using this method. Using this method. The concrete overlay procedure involves adding a sufficient layer of concrete as a coating over an existing reinforced concrete section using longitudinal and transverse ties. The concrete and reinforcement This additional concrete and reinforcement increase strength and stiffness. It may require considerable puncturing into existing columns. The added longitudinal bars must be anchored to the foundation and made continuous through the slab if present in the original structure. This process requires drilling holes in the existing columns, slabs, beams, and foundations. Precast concrete coatings are also available today, offering customised designs and installation techniques for faster construction [55].

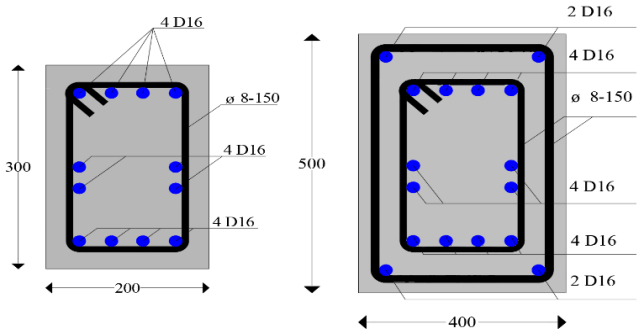

Fig. 15. Comparison of reinforced concrete for the beam before and after retrofitting.

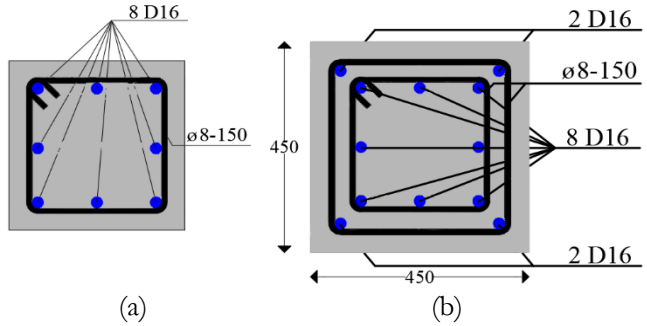

Fig. 16. Comparison of reinforced concrete for the column before and after retrofitting.

However, since most FRP material production is conducted overseas, their prices tend to be higher. Instead of FRP, ferrocement—a mixture of mortar and fine mesh—can also be considered. Ferrocement has similarities with FRP and can be a more economical option when fibre technology is applied to building structures. Figure 17 presents the stress ratio after retrofitting. It can be seen that there is no further weakening in the column and its surroundings. The main objective of repairing and strengthening structures is to achieve adequate strength and comply with design standards for earthquake planning. Figure 18 illustrates the internal force after retrofitting.

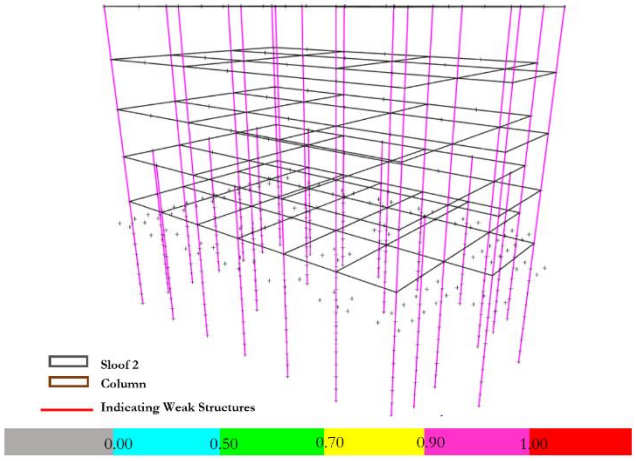

Fig. 17. Stress ratio after retrofit.

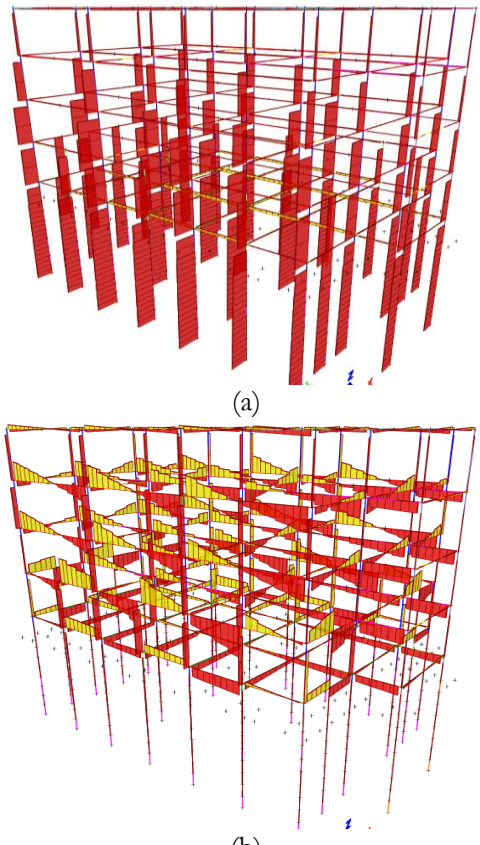

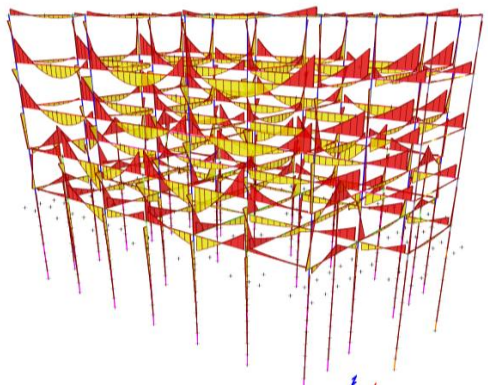

(c)

Fig. 18. Internal forces after retrofitting, (a) normal forces, (b) shear forces, (c) bending moment.

Retrofitting is still possible even for future strong earthquakes, provided that the technical design is adapted to the worst-case earthquake scenario and that regulatory support, funding, and community participation are also in place. Without retrofitting, the study area risks greater infrastructure destruction and loss of life. Investing today will save thousands of lives and economic assets in the future.

5. Conclusion

This study utilises ground motion evaluations and structural dynamics analysis to assess the Integrated Laboratory Building at the Faculty of Engineering, University of Bengkulu, during a significant megathrust earthquake. Key findings from the studies are:

1. Data such as earthquake acceleration time history and amplification factors can support further investigations, particularly in evaluating soil-structure interaction. This study differs from previous studies in that it compares the values of peak ground acceleration (PGA), peak ground displacement (PGV), and peak ground velocity (PGD) at the surface, pile tip, and input motion, and obtains an amplification factor value of 1.430.
2. Dynamic analysis of the site, utilising field-collected data, reveals that the soil is predominantly sand. The ground surface's spectral acceleration corresponds well to the seismic design code requirements, confirming the building's compliance with regulatory standards. Therefore, buildings constructed according to the seismic design code are relatively safe during earthquake-induced shaking.
3. After inputting the time history of earthquake acceleration, the structural behaviour assessment outcomes detected several red-coloured elements and O/S, indicating that the building structure has exceeded its capacity (overstrength) or is unsafe. The weakening occurred in column 3, located on the first floor, with dimensions of 25 × 25 cm; this is because column 3 is only on the first floor and directly supports the load above it. In addition, Sloof 2, with dimensions of 20 × 30 cm, also weakened because the beam could not withstand the given load.
4. Building inspections are essential for evaluating buildings' seismic performance, allowing for follow-up measures to minimise potential damage and the consequences of a significant earthquake. Solutions to structural damage can be implemented through retrofitting methods that enhance the performance of columns and slabs.
5. Although this study is based on a regional case in Bengkulu, Indonesia, the methodological approach used — combining nonlinear soil response analysis and structural dynamics within the PBEE framework — has the potential to be widely adopted in other seismic regions. Therefore, the findings and methods in this study are expected to contribute to earthquake engineering practice at the international level, especially in areas with similar soil characteristics and subduction activity.
6. Earthquakes can trigger a ground failure phenomenon known as liquefaction. Therefore, it is essential to analyse the liquefaction potential by considering the seismic response of the soil [56]. Liquefaction itself is a geotechnical phenomenon that occurs as a direct result of earthquake activity, causing severe damage to buildings that are susceptible to liquefaction. In assessing liquefaction potential, it is essential to pay attention to the duration of shaking, as high ground accelerations and long shaking durations can prolong the duration of liquefaction and increase the risk [57].

Acknowledgements

The researchers acknowledge the support and resources provided by the Department of Civil Engineering, Faculty of Engineering, University of Bengkulu, for funding this study. They would like to thank the Integrated Laboratory of the Faculty of Engineering for providing the essential data used in this research. First author (N.R. Handayani) acknowledges the Geotechnical Hazard Research Unit (Dr. Mase's Laboratory) for their assistance in conducting the analysis and writing the manuscript.

References

[1] Y. Haryanto, H.-T. Hu, A. L. Han, B. A. Hidayat, A. Widyaningrum, and P. E. Yulianita, "Seismic vulnerability assessment using rapid visual screening: Case study of educational facility buildings of Jenderal Soedirman University, Indonesia," *Civil Engineering Dimension*, vol. 22, no. 1, pp. 13–21, May 2020, doi: 10.9744/ced.22.1.13-21.

[2] L. Z. Mase, "Seismic vulnerability maps of Ratu Agung District, Bengkulu City, Indonesia," *Civil Engineering Dimension*, vol. 21, no. 2, pp. 97–106, Oct. 2019, doi: 10.9744/ced.21.2.97-106.

[3] L. Z. Mase, D. Gustina, A. Zahara, F. Supriani, S. Chaiyaput, and A. J. Syahbana, "The joint method of ground response and structural dynamic analyses for building inspection under a large megathrust earthquake," *Transportation Infrastructure Geotechnology*, vol. 12, no. 1, Jan. 2025, doi: 10.1007/s40515-024-00480-w.

[4] L. Z. Mase, S. Isdianty, and K. Amri, "Numerical analyses to observe the performance of a monumental building at the University of Bengkulu, Indonesia," *Rudarsko Geolosko Naftni Zbornik*, vol. 39, no. 4, pp. 23–39, 2024, doi: 10.17794/rgn.2024.4.3.

[5] L. Z. Mase, K. Amri, F. Rahmat, M. N. Fikri, J. Saputra, and S. Likitlersuang, "Effect of water level fluctuation on riverbank stability at the estuary area of Muaro Kualo Segment, Muara Bangkahulu River in Bengkulu, Indonesia." *Engineering Journal*, vol. 26, no. 3, pp. 1–16, 2022, doi: 10.4186/ej.2022.26.3.1.

[6] G. M. Sapidis, M. C. Naoum, N. A. Papadopoulos, E. Golias, C. G. Karayannis, and C. E. Chalioris, "A novel approach to monitoring the performance of carbon-fiber-reinforced polymer retrofitting in reinforced concrete beam–column joints," *Applied Sciences (Switzerland)*, vol. 14, no. 20, Oct. 2024, doi: 10.3390/app14209173.

[7] O. B. Putra, I. D. Ramadhan, A. Rosyidah, J. Saputra, and I. K. Sucita, "Investigation of seismic resistant structures with various moment-resisting frame systems and pushover analysis," *Sinergi (Indonesia)*, vol. 28, no. 3, pp. 535–544, 2024, doi: 10.22441/sinergi.2024.3.010.

[8] P. Pudjisuryadi, B. Lumantarna, T. F. Hermawan, and T. T. Gunawan, "Seismic performance of existing building retrofitted with VSL-Gensui damper," *Civil Engineering Dimension*, vol. 20, no. 2, pp. 86–90, Oct. 2018, doi: 10.9744/ced.20.2.86-90.

[9] R. Misliniyati, L. Z. Mase, M. Irsyam, Hendriyawan, and A. Sahadewa, "Seismic response validation of simulated soil models to vertical array record during a strong earthquake," *Journal of Engineering and Technological Sciences*, vol. 51, no. 6, pp. 772–790, 2019, doi: 10.5614/j.eng.technol.sci.2019.51.6.3.

[10] L.Z. Mase, R. Yundrismein, M. A. Nursalam, S. M. Putra, A. Shelina, and S. H. Nugroho, "A study of building performance inspection based on a combination of site-specific response analysis and structural analysis (A case study of the Lighthouse View Tower in Bengkulu City, Indonesia)," *Rudarsko Geolosko Naftni Zbornik*, vol. 37, no. 3, pp. 197–209, Jun. 2022, doi: 10.17794/rgn.2022.3.14.

[11] A. M. Zapata-Franco, Y. F. Vargas-Alzate, J. M. Gonzalez, and E. B. Olmos-Toledo, "FEM-based spectral matching to obtain specific surface spectra," *Soil Dynamics and Earthquake Engineering*, vol. 190, Mar. 2025, doi: 10.1016/j.soildyn.2024.109153.

[12] L. Z. Mase, S. Likitlersuang, and T. Tobita, "Non-linear Site Response Analysis of Soil Sites in Northern Thailand during the M_w 6.8 Tarlay Earthquake," *Engineering Journal*, vol. 22, doi: 10.4186/ej.2018.22.3.289.

[13] Y. Cho, S. Ahn, J. Lee, J. Kim, B. Kim, and S. Jeong, "Characteristics of ground motions in the Jeju Island during the 2021 Ml4.9 Jeju earthquake, South Korea," *KSCE Journal of Civil Engineering*, p. 100148, Dec. 2024, doi: 10.1016/j.kscej.2024.100148.

[14] L. Makrup, W. Pawirodikromo, and Y. Muntafi, "Comparison of structural response utilizing probabilistic seismic hazard analysis and design spectral ground motion," *Civil Engineering Journal*, vol. 10, pp. 235–251, Dec. 2024, doi: 10.28991/CEJ-SP2024-010-012.

[15] M. R. Shendkar, D. P. N. Kontoni, S. Mandal, P. R. Maiti, and O. Tavasoli, "Seismic evaluation and retrofit of reinforced concrete buildings with masonry infills based on material strain limit approach," *Shock and Vibration*, vol. 2021, 2021, doi: 10.1155/2021/5536409.

[16] S. Ghaffarian and S. Emtehani, "Monitoring urban deprived areas with remote sensing and machine learning in case of disaster recovery," *Climate*, vol. 9, no. 4, Apr. 2021, doi: 10.3390/cli9040058.

[17] F. Foroughnia, V. Macchiarulo, L. Berg, M. DeJong, P. Milillo, K. W. Hudnut, K. Gavin. And G. Giardina "Quantitative assessment of earthquake-induced building damage at regional scale using LiDAR data," *International Journal of Disaster Risk Reduction*, vol. 106, May 2024, doi: 10.1016/j.ijdrr.2024.104403.

[18] M. R. Shendkar, A. Tantri, and A. U. Rao, "Seismic evaluation and retrofit of reinforced concrete structures," *Journal of Infrastructure Preservation and Resilience*, vol. 6, no. 1, p. 2, Jan. 2025, doi: 10.1186/s43065-024-00114-y.

[19] P. Pudjisuryadi, B. Lumantarna, R. Setiawan, and C. Handoko, "Performance of an existing reinforced concrete building designed in accordance to older Indonesian Seismic Code: A case study for a hotel in Kupang, Indonesia," *Civil Engineering Dimension*, vol. 20, no. 1, pp. 35–40, Apr. 2018, doi: 10.9744/ced.20.1.35-40.

[20] P. Blagojević, S. Brzev, and R. Cvetković, "Seismic retrofitting of mid-rise unreinforced masonry residential buildings after the 2010 Kraljevo, Serbia Earthquake: A case study," *Buildings*, vol. 13, no. 3, Mar. 2023, doi: 10.3390/buildings13030597.

[21] M. C. Naoum, N. A. Papadopoulos, G. M. Sapidis, and C. E. Chalioris, "Advanced structural monitoring technologies in assessing the performance of retrofitted reinforced concrete elements," *Applied Sciences (Switzerland)*, vol. 14, no. 20, Oct. 2024, doi: 10.3390/app14209282.

[22] K. R. Mackie, J. Lu, and A. Elgamal, "Performance-based earthquake assessment of bridge systems including ground-foundation interaction," *Soil Dynamics and Earthquake Engineering*, vol. 42, pp. 184–196, Nov. 2012, doi: 10.1016/j.soildyn.2012.05.023.

[23] L. Z. Mase, N. Sugianto, and Refrizon, "Seismic hazard microzonation of Bengkulu City, Indonesia,"

Geoenvironmental Disasters, vol. 8, no. 1, Dec. 2021, doi: 10.1186/s40677-021-00178-y.

[24] L. Z. Mase, W. Tanapalungkorn, S. Likitlersuang, K. Ueda, and T. Tobita, "Liquefaction analysis of Izumio sands under variation of ground motions during strong earthquake in Osaka, Japan," *Soils and Foundations*, vol. 62, no. 5, Oct. 2022, doi: 10.1016/j.sandf.2022.101218.

[25] T. S. Nguyen, K. Ngamcharoen, and S. Likitlersuang, "Statistical characterisation of the geotechnical properties of Bangkok subsoil," *Geotechnical and Geological Engineering*, vol. 41, no. 3, pp. 2043–2063, May 2023, doi: 10.1007/s10706-023-02390-z.

[26] R. Sukkarak, W. Tanapalungkorn, S. Likitlersuang, and K. Ueda, "Liquefaction analysis of sandy soil during strong earthquake in Northern Thailand," *Soils and Foundations*, vol. 61, no. 5, pp. 1302–1318, Oct. 2021, doi: 10.1016/j.sandf.2021.07.003.

[27] L. Z. Mase, W. Tanapalungkorn, P. Anussornrajkit, and S. Likitlersuang, "Assessing liquefaction risk and hazard mapping in a high-seismic region: A case study of Bengkulu City, Indonesia," *Natural Hazards*, Apr. 2024, doi: 10.1007/s11069-024-07057-3.

[28] L. Z. Mase, K. Amri, K. Ueda, R. Apriani, F. Utami, T. Tobita, S. Likitlersuang, "Geophysical investigation on the subsoil characteristics of the Dendam Tak Sudah Lake site in Bengkulu City, Indonesia," *Acta Geophysica*, vol. 72, no. 2, pp. 893–913, Apr. 2024, doi: 10.1007/s11600-023-01158-6.

[29] T. S. Nguyen, T. N. Phan, S. Likitlersuang, and D. T. Bergado, "Characterization of stationary and nonstationary random fields with different copulas on undrained shear strength of soils: Probabilistic analysis of embankment stability on soft ground," vol. 22, no. 7, p. 04022109, 2022, doi: 10.1061/(ASCE).

[30] T. S. Nguyen, S. Likitlersuang, W. Tanapalungkorn, T. N. Phan, and S. Keawsawasvong, "Influence of copula approaches on reliability analysis of slope stability using random adaptive finite element limit analysis," *Int J Numer Anal Methods Geomech*, vol. 46, no. 12, pp. 2211–2232, Aug. 2022, doi: 10.1002/nag.3385.

[31] T. S. Nguyen and S. Likitlersuang, "Influence of the spatial variability of soil shear strength on deep excavation: A case study of a Bangkok underground MRT Station," *International Journal of Geomechanics*, vol. 21, no. 2, Feb. 2021, doi: 10.1061/(asce)gm.1943-5622.0001914.

[32] T. S. Nguyen, W. Tanapalungkorn, S. Keawsawasvong, V. Q. Lai, and S. Likitlersuang, "Probabilistic analysis of passive trapdoor in c-ϕ soil considering multivariate cross-correlated random fields," *Geotechnical and Geological Engineering*, vol. 42, no. 3, pp. 1849–1869, May 2024, doi: 10.1007/s10706-023-02649-5.

[33] L. Z. Mase, S. Isdianty, and K. Amri, "Numerical analyses to observe the performance of a monumental building at the University of Bengkulu, Indonesia," *Rudarsko Geolosko Naftni Zbornik*, vol. 39, no. 4, pp. 23–39, 2024, doi: 10.17794/rgn.2024.4.3.

[34] L. Z. Mase, J. Saputra, A. F. Edriani, S. Keawsawasvong, and V. Q. Lai, "Finite element analysis to estimate bearing capacity of strip footing in coastal sandy soils in Bengkulu City, Indonesia," *Engineering Journal*, vol. 26, no. 5, pp. 59–75, May 2022, doi: 10.4186/ej.2022.26.5.59.

[35] L. Z. Mase, D. Gustina, A. Zahara, F. Supriani, S. Chaiyaput, and A. J. Syahbana, "The joint method of ground response and structural dynamic analyses for building inspection under a large megathrust earthquake," *Transportation Infrastructure Geotechnology*, vol. 12, no. 1, Jan. 2025, doi: 10.1007/s40515-024-00480-w.

[36] O. Arroyo, A. Liel, and S. Gutiérrez, "A performance-based evaluation of a seismic design method for reinforced concrete frames," *Journal of Earthquake Engineering*, vol. 22, no. 10, pp. 1900–1917, Nov. 2018, doi: 10.1080/13632469.2017.1309605.

[37] I. Choi, H.Y. Lee, and B.K. Oh, "Convolutional neural network-based seismic response prediction method using spectral acceleration of earthquakes and conditional vector of structural property," *Soil Dynamics and Earthquake Engineering*, vol. 187, Dec. 2024, doi: 10.1016/j.soildyn.2024.109021.

[38] S. Ghimire, P. Guéguen, and A. Astorga, "Analysis of the efficiency of intensity measures from real earthquake data recorded in buildings," *Soil Dynamics and Earthquake Engineering*, vol. 147, Aug. 2021, doi: 10.1016/j.soildyn.2021.106751.

[39] L.R. Poreddy, M. K. Pathapadu, C. Navyatha, J. Vemuri, and R. Chenna, "Correlation analysis between ground motion parameters and seismic damage of buildings for near-field ground motions," *Natural Hazards Research*, vol. 2, no. 3, pp. 202–209, Sep. 2022, doi: 10.1016/j.nhres.2022.08.002.

[40] J. Carrillo, O. Arroyo, and S. M. Alcocer, "Damage indexes for performance assessment of low-rise reinforced concrete walls," in *Seismic Evaluation, Damage, and Mitigation in Structures*, Elsevier, 2022, pp. 3–16. doi: 10.1016/B978-0-323-88530-0.00008-8.

[41] L. Z. Mase, W. Tanapalungkorn, K. Ueda, and S. Likitlersuang, "Non-linear site response analysis of liquefaction in the port area of Bengkulu City due to large subduction earthquakes," *Transportation Infrastructure Geotechnology*, vol. 12, no. 2, Feb. 2025, doi: 10.1007/s40515-025-00540-9.

[42] L. Z. Mase, "Seismic hazard vulnerability of Bengkulu City, Indonesia, based on deterministic seismic hazard analysis," *Geotechnical and Geological Engineering*, vol. 38, no. 5, pp. 5433–5455, Oct. 2020, doi: 10.1007/s10706-020-01375-6.

[43] A. I. Hadi, M. Farid, L. Z. Mase, Refrizon, S. B. Purba, D. I. Fadli, and E. Sumanjaya, "Zonation of seismic vulnerability levels in South Bengkulu Regency, Indonesia for disaster-based regional planning," *Rudarsko Geolosko Naftni Zbornik*, vol. 39,

no. 2, pp. 133–148, Apr. 2024, doi: 10.17794/rgn.. 2024.2.11.

[44] L. Z. Mase, S. Agustina, H. Hardiansyah, M. Farid, F. Supriani, W. Tanapalungkorn, S. Likitlersuang, "Application of simplified energy concept for liquefaction prediction in Bengkulu City, Indonesia," *Geotechnical and Geological Engineering*, vol. 41, no. 3, pp. 1999–2021, May 2023, doi: 10.1007/s10706-023-02388-7.

[45] N. Gunawan, A. Han, and B. S. Gan, "Proposed design philosophy for seismic-resistant buildings," *Civil Engineering Dimension*, vol. 21, no. 1, pp. 1–5, Mar. 2019, doi: 10.9744/ced.21.1.1-5.

[46] R. Misliniyati, L. Z. Mase, A. J. Syahbana, and E. Soebowo, "Seismic hazard mitigation for Bengkulu Coastal area based on site class analysis," in *IOP Conference Series: Earth and Environmental Science*, Institute of Physics Publishing, Dec. 2018. doi: 10.1088/1755-1315/212/1/012004.

[47] M. F. Qodri, L. Z. Mase, and S. Likitlersuang, "Non-linear site response analysis of Bangkok subsoils due to earthquakes triggered by three pagodas fault," *Engineering Journal*, vol. 25, no. 1, pp. 43–52, 2021, doi: 10.4186/ej.2021.25.1.43.

[48] K. Leng, C. Chintanapakdee, and T. Hayashikawa, "Seismic shear forces in shear walls of a medium-rise building designed by response spectrum analysis," *Engineering Journal*, vol. 18, no. 4, pp. 73–95, Oct. 2014, doi: 10.4186/ej.2014.18.4.73.

[49] L. Z. Mase, "A case study of liquefaction potential verification during a strong earthquake at Lempuing Subdistrict, Bengkulu City, Indonesia," *Transportation Infrastructure Geotechnology*, vol. 11, no. 4, pp. 1547–1572, Aug. 2024, doi: 10.1007/s40515-023-00335-w.

[50] M. Bahrampouri, A. Rodriguez-Marek, S. Shahi, and H. Dawood, "An updated database for ground motion parameters for KiK-net records," *Earthquake Spectra*, vol. 37, no. 1, pp. 505–522, Feb. 2021, doi: 10.1177/8755293020952447.

[51] R. Misliniyati, L. Z. Mase, Refrizon, W. D. Primaningtyas, Z. Fahrezi, A. Zahara, G. D. Anggraini, and E. Y. Sari. "Liquefaction risk assessment and microzonation in bengkulu port area after a megathrust earthquake," *Geotechnical and Geological Engineering*, vol. 43, no. 3, Mar. 2025, doi: 10.1007/s10706-025-03090-6.

[52] L. Z. Mase, W. Tanapalungkorn, S. Likitlersuang, K. Ueda, and T. Tobita, "Ground motion, liquefaction and hazard analysis at the Palu site during the 2018 Indonesian great earthquake," *China Geology*, vol. 8, no. 0, pp. 1–23, 2025, doi: 10.31035/cg20240065.

[53] M. F. Qodri, V. D. A. Anggorowati, and L. Z. Mase, "Site-specific analysis to investigate response and liquefaction potential during the megathrust earthquake at Banten Province Indonesia," *Engineering Journal*, vol. 26, no. 9, pp. 1–10, 2022, doi: 10.4186/ej.2022.26.9.1.

[54] M. S. Lee and L. H. Lee, "Hysteresis behavior of reinforced concrete column retrofitted and repaired with carbon fiber sheet," *Int J Concr Struct Mater*, vol. 19, no. 1, p. 1, Feb. 2025, doi: 10.1186/s40069-024-00748-y.

[55] G. R. Reddy, D. K. Jha, and G. Verma, "Retrofitting of structures and equipments," in *Textbook of Seismic Design*. Springer Singapore, 2019, pp. 457–519. doi: 10.1007/978-981-13-3176-3_13.

[56] L. Z. Mase and S. Likitlersuang, "Implementation of seismic ground response analysis in estimating liquefaction potential in Northern Thailand," *Indonesian Journal on Geoscience*, vol. 8, no. 3, pp. 371–383, Dec. 2021, doi: 10.17014/ijog.8.3.371-383

[57] L. Z. Mase, T. Faisal Fathani, and A. Darmawan Adi, "A simple shaking table test to measure liquefaction potential of Prambanan Area, Yogyakarta, Indonesia," *ASEAN Engineering Journal*, vol. 11, no. 3, pp. 89-108, Sept 2021. doi.org: 10.11113/aej.v11.16874

Nur Rahman Handayani, photograph and biography not available at the time of publication.

Lindung Zalbuin Mase, photograph and biography not available at the time of publication.

Sahrul Hari Nugroho, photograph and biography not available at the time of publication.

Fepy Supriani, photograph and biography not available at the time of publication.

Rena Misliniyati, photograph and biography not available at the time of publication.

Khairul Amri, photograph and biography not available at the time of publication.